Making deep mutational scanning accessible: a cost-efficient approach to construct barcoded libraries for genes of any length

Jessica Jann[1-4], Isabelle Gagnon-Arsenault[1-4], Alicia Pageau[1-4], Alexandre K Dubé[1-4], Anna Fijarczyk[1-4], Romain Durand[1-4], Christian R. Landry*[1-4]

Affiliations:
[1]Département de biochimie, de microbiologie et de bio-informatique, Faculté des sciences et de génie, Université Laval, G1V 0A6, Québec, Canada
[2]Institut de biologie intégrative et des systèmes, Université Laval, G1V 0A6, Québec, Canada
[3]PROTEO, Le regroupement québécois de recherche sur la fonction, l'ingénierie et les applications des protéines, Université Laval, G1V 0A6, Québec, Canada
[4]Centre de recherche sur les données massives, Université Laval, G1V 0A6, Québec, Canada

*Correspondence to Christian.landry@bio.ulaval.ca

Abstract

Recent developments in DNA synthesis and sequencing have allowed the construction of comprehensive gene variant libraries and their functional analysis. Achieving high-replication and thorough mutation characterization remains technically and financially challenging for long genes. Here, we developed an efficient, affordable and scalable library construction approach that relies on low-cost DNA synthesis and standard cloning technologies, which will increase accessibility to systematic mutational studies and help advance the field of protein science.

Main text

Understanding how genetic variation alters protein function is a central goal in genetics, molecular biology, and evolutionary and biomedical research. Over the past decade, Deep Mutational Scanning (DMS) has emerged as a powerful technology to systematically evaluate the functional consequences of all possible single amino acid substitutions in a protein within a single experiment [1,2]. By coupling a comprehensive variant library, selection assays, and high-throughput sequencing, DMS allows the systematic quantification and mapping of genotype–phenotype relationships at high resolution and coverage [1,2].

DMS involves four major steps: (i) the construction of a comprehensive variant library, typically introducing all possible single amino acid substitutions into a target gene (or specific locus); (ii) the delivery of this library into a biological system via vectors (such as plasmids) or genomic integration; (iii) the application of a selective pressure (e.g., drug exposure, receptor activation, protein stability challenge); and (iv) the quantification of variant frequencies before and after selection using deep sequencing, allowing the estimation of functional effects for each single substitution. These mutational landscapes provide insights into structure-function relationships, disease-associated mutations, and evolutionary mechanisms.

The robustness and completeness of a DMS experiment lie in the quality and design of the variant library. Constructing a systematic variant library offers several advantages over random or non-systematic approaches (e.g., error-prone PCR) [3,4]. It ensures exhaustive mutational coverage and removes biases introduced by targeted or region-focuses mutagenesis. Furthermore, vector-based variant libraries offer flexibility in downstream applications: they can be easily stored and reused in different genetic backgrounds or biological systems [5], coupled with fluorescent tags or reporters [6], and they allow flexible expression under inducible or constitutive promoters [7]. Vector-based libraries can be used not only for transformation but also as templates for transferring mutations into genomic loci using CRISPR-Cas9 or homologous recombination [8,9]. Examples of vector-based DMS applications include signaling-specific variants of MC4R in obesity [10], immune escape mutations in the SARS-CoV-2 Spike protein [11], and pathogenicity classifications for CRX and PAX6 in inherited eye disorders [12]. In microbes, recent efforts have used DMS to map resistance-conferring mutations [13].

While DMS is a powerful tool for high-throughput functional analysis, generating reproducible and high-coverage data remains challenging. Incorporating internal replicates, such as multiple unique codons or DNA barcodes per amino acid variant, reduces technical noise, improves the precision of effect estimates, and enhances sensitivity and reproducibility [14–16] Plasmid-based libraries further facilitate this design by linking each variant to unique short DNA barcodes, enabling cost-effective tracking of mutation frequencies across diverse conditions using short-read sequencing.

Although the cost of high-throughput sequencing has steadily declined over the past 20 years, the large size of many target genes makes the cost of such experiments prohibitive. Gene size limits DMS scalability due to the complexity of the variant library and the associated synthesis and sequencing costs. To overcome these challenges, we developed an efficient and cost-

effective two-step cloning strategy for plasmid-based DMS libraries that facilitates the study of large genes using DNA-barcoded synthetic oligonucleotide variants.

Our approach involves fragmenting the gene of interest (*Your Favorite Gene: YFG*) into subregions of up to 150 bp, in accordance with the synthesis length limits of single-stranded oligonucleotide pools (oPools) (Figure 1A). Plasmid libraries are constructed fragment-by-fragment to simplify the cloning strategy, facilitate variant tracking, and minimize diversity loss throughout the process. For each fragment, a variant library is built using affordable single-stranded DNA fragments containing three components:

I. a *YFG* fragment sequence containing a single NNK codon substitution;
II. BsaI restriction sites for modular assembly; and
III. a 30 bp DNA barcode alternating random dinucleotides (NN) with codon position-specific sequences.

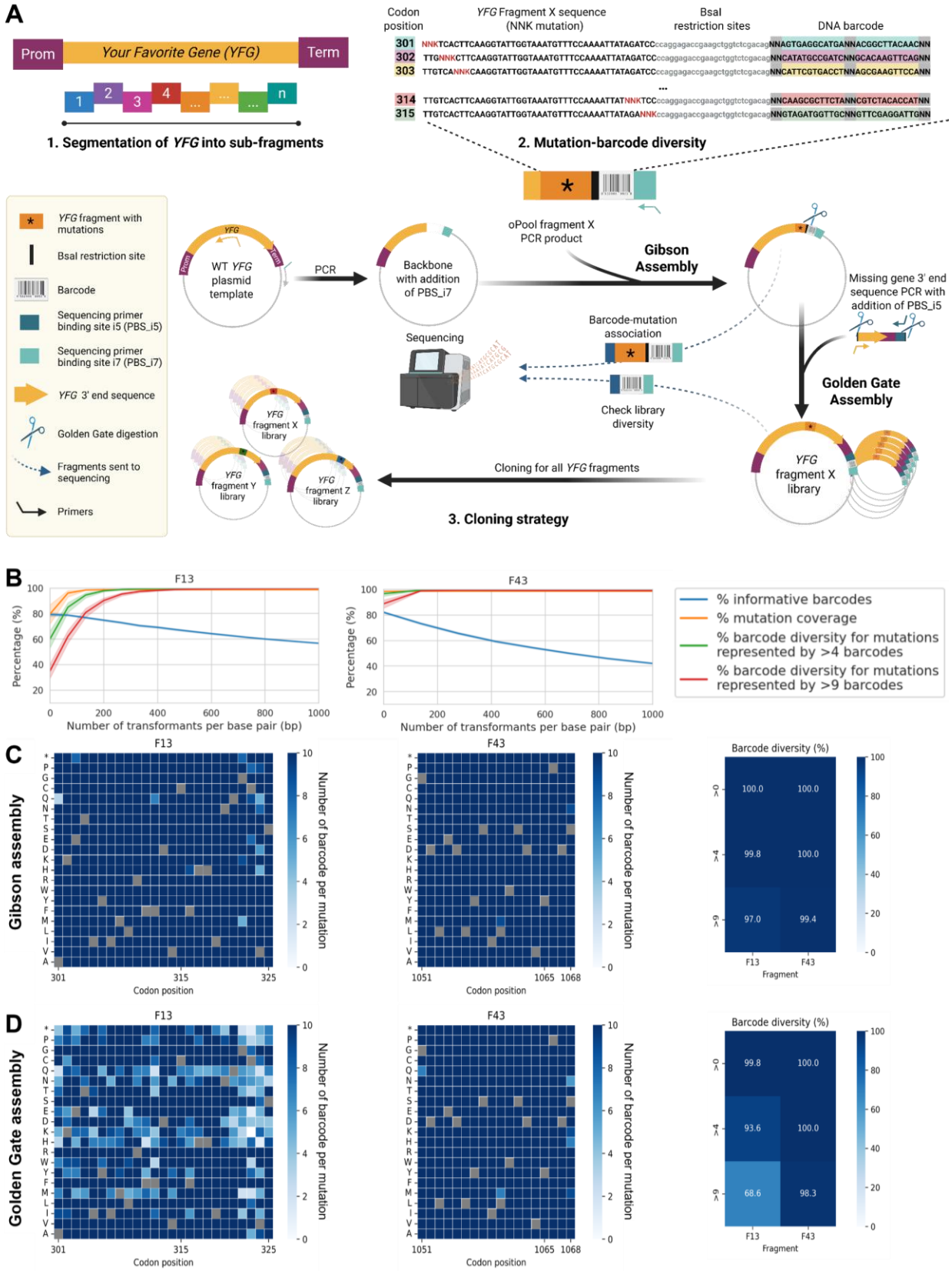
A
Prom
Your Favorite Gene (YFG)
Term
1. Segmentation of YFG into sub-fragments
Codon position
YFG Fragment X sequence (NNK mutation)
BsaI restriction sites
DNA barcode
2. Mutation-barcode diversity
YFG fragment with mutations
BsaI restriction site
Barcode
Sequencing primer binding site i5 (PBS_i5)
Sequencing primer binding site i7 (PBS_i7)
YFG 3' end sequence
Golden Gate digestion
Fragments sent to sequencing
Primers
WT YFG plasmid template
PCR
Backbone with addition of PBS_i7
oPool fragment X PCR product
Gibson Assembly
Missing gene 3' end sequence PCR with addition of PBS_i5
Sequencing
Barcode-mutation association
Check library diversity
Golden Gate Assembly
YFG fragment X library
YFG fragment Y library
YFG fragment Z library
Cloning for all YFG fragments
3. Cloning strategy
B
F13
F43
Percentage (%)
Number of transformants per base pair (bp)
% informative barcodes
% mutation coverage
% barcode diversity for mutations represented by >4 barcodes
% barcode diversity for mutations represented by >9 barcodes
C
Gibson assembly
Number of barcode per mutation
Codon position
Barcode diversity (%)
Fragment
100.0
100.0
99.8
100.0
97.0
99.4
D
Golden Gate assembly
99.8
100.0
93.6
100.0
68.6
98.3

Figure 1 - A) Strategy to generate a DMS plasmid library for *Your Favorite Gene* (*YFG*) using short, degenerate libraries. 1. Segmentation of YFG into sub-fragments, each fragment corresponding to a DNA region to be synthesized. The same approach can be applied to promoter and terminator regions, if desired. **2.** Example of an affordable pool of degenerate oligonucleotides (oPool) from one *YFG* fragment associated with DNA barcodes. Each oPool contains the *YFG* fragment sequence with a single NNK codon, the BsaI cloning sites, and a DNA barcode composed of codon-position specific regions and six degenerate nucleotides (N). Current technologies allow for nine degenerate positions per fragment. Three are used for the degenerate codon (NNK), and six for the barcode. **3.** Protocol for constructing *YFG* DMS plasmid library from oPools using two cloning steps that maintain the physical barcode-mutation association. The degenerate gene fragments and the associated barcodes are cloned into the plasmid template by Gibson cloning, adding a Primer Binding Site_i7 (PBS_i7) sequence. Following this step, short read sequencing using PBS_i5 (included in the 5' sequencing primer) and PBS_i7 is performed to associate barcodes with the degenerate codon for each fragment and to assess both mutation coverage and barcode diversity per mutation. The ultimate step consists in Golden Gate cloning of the missing 3' gene fragment between the degenerate fragment and the barcode. An additional short read sequencing step of the barcodes can be performed to make sure that coverage and diversity has been maintained. **B) Optimisation of cloning steps.** Cumulative percentage of informative barcodes (those associated with a single coding mutation and not with the WT), mutation coverage (percentage of mutations represented by at least one informative barcode) and barcode diversity (percentage of informative barcodes per coding mutation) as a function of the number of transformants recovered after Gibson cloning for two fragments (F13 and F43) of a long gene coding for a transcription factor. Means and confidence intervals obtained for 100 random draws of transformation reactions. **Library quality control after (C) Gibson and (D) Golden Gate assemblies for *PDR1* F13 and F43**. Heatmaps show barcode diversity for each possible amino acid substitution at each codon position. For each fragment, a total of 25,000 and 100,000 transformants were recovered and analyzed after Gibson and Golden Gate assemblies, respectively. Covered mutations are represented by a barcode diversity >0, while a barcode diversity threshold of >4 or >9 demonstrates an increasing number of replicates for a same mutation. Grey squares represent wild-type (WT) amino acids.

The barcode design facilitates variant identification while allowing each amino acid substitution to be represented by multiple distinct barcodes, thereby providing internal replicates for downstream analysis. The barcodes and their corresponding variants remain physically linked on the same DNA molecule (plasmid), ensuring accurate tracking throughout the experiment. All oPools are flanked by a 3′ Primer Binding Site_i7 (PBS_i7) for rapid and efficient sequencing library preparation.

This strategy utilizes the cost-efficiency of oPools, which are ~100-fold cheaper per base than double-stranded DNA synthesis (<$0.001 vs. ~$0.05 per base) [17,18]. In addition, low-cost short-read sequencing is used (i) to associate random barcodes to their corresponding coding sequence variants and (ii) to track mutations in downstream experiments via the barcodes. This approach offers a cost-effective alternative to methods that require long-read sequencing to variant identification and tracking [19,20]. A cost comparison of different DMS library construction strategies (saturation mutagenesis, commercial synthesis, etc.) highlights the financial advantage of our approach (Supplementary Table A and Supplementary Figure 1). Notably, the initial library's low-cost per amino acid position remains constant regardless of gene length, unlike other strategies where costs increase substantially with gene size (Supplementary Figure 1).

The cloning strategy is divided into two steps: a Gibson assembly, followed by a Golden Gate assembly (Figure 1A). In the first step, the plasmid backbone is generated via PCR from a yeast expression vector containing the wild-type (WT) *YFG*. Gibson assembly allows inserting the oPools (variant fragment + barcode + PBS_i7) into the backbone. These constructs then serve as backbone plasmids for the second cloning step.

In the second step, the missing *YFG* 3′ end sequence is amplified, including the C-terminal coding region, terminator, and PBS_i5. Golden Gate assembly enables the one-pot assembly of this missing *YFG* 3′ end sequence into the Gibson-assembled plasmids, using BsaI digestion and vector-insert ligation cycles (see *methods* section). This strategy results in one distinct plasmid library per *YFG* fragment, each containing a full-length *YFG* sequence carrying a single mutation (in the targeted fragment) specifically linked to a DNA barcode flanked by the PBS_i5 and PBS_i7.

Each library undergoes quality control by high-throughput sequencing at both cloning steps (Figure 1):

- After Gibson assembly, short-read sequencing (mutated fragment + barcode) is used to (i) establish barcode–mutation associations and (ii) assess both mutation coverage and barcode diversity per mutation.
- After Golden Gate assembly, only the DNA barcodes require to be sequenced to confirm that coverage and diversity have been maintained.

To demonstrate the feasibility and the strength of our approach, DMS libraries for two fragments (F13 and F43) of a long gene coding for a transcription factor were constructed and characterized (Figure 1B, C and D). We focused on these two fragments because they cover a wide range and distances from the DNA barcodes and F13 contains mutations of interest. The performance of a DMS plasmid library depends on three key parameters: Informative barcodes (i.e., barcodes associated with only one coding mutation and not with the WT), which ensure data usability and limit sequencing costs of non informative barcodes; Mutation coverage (i.e., the number of mutations represented by at least one informative barcode); Barcode diversity (i.e., number of informative barcodes per mutation), which provides internal replicates.

These parameters are largely dependent on the number of recovered transformants after each cloning step. A random sampling of their distribution indicates that after Gibson assembly, ~350 transformants per base pair (bp) are needed to optimize sufficient mutation coverage, barcode diversity, and informative barcode (Figure 1B). This level of recovery yields 300-350 informative barcodes covering all possible mutations, with over 99.8% of mutations represented by >4 barcodes and over 97.0% by >9 barcodes (Figure 1B and C). These results demonstrate excellent mutation coverage and barcode diversity, two essential features for the robustness and reproducibility of DMS data.

As each cloning step inevitably results in some diversity loss, the number of transformants recovered after Golden Gate assembly was increased fourfold (~1400 transformants per bp). Although a small subset of mutations showed lower representation, our cloning strategy ensured

over 99.8% of mutation coverage and preserved high barcode diversity: over 93.6% of mutations were still covered by >4 barcodes, and over 68.6% by >9 barcodes (Figure 1D).

To demonstrate the feasibility and utility of our cloning strategy, we focused on antifungal resistance, an increasingly pressing issue due to the rising incidence of invasive fungal infections and the limited number of effective treatment options [21]. Drug resistance mutations significantly compromise the efficacy of antifungal therapies, underscoring the urgent need for innovative approaches to investigate and counteract resistance mechanisms [22]. Among current antifungal drugs, azoles are widely used in clinical settings, including posaconazole, a broad-spectrum triazole [23–26]. The transcription factor Pleiotropic Drug Resistance 1 (Pdr1) plays a key role in mediating multidrug resistance [27]. Mutations in *PDR1* lead to overexpression of downstream targets, including ABC efflux pump genes like *CDR1, CDR2,* and *SNQ2*, conferring broad-spectrum drug resistance in both the model yeast *Saccharomyces cerevisiae* and the human pathogen *Nakaseomyces glabratus (Candida glabrata)* [28,29]. Although numerous studies have demonstrated the central role of *PDR1*, the precise identity and functional impact of resistance-conferring mutations remain largely unknown. Thus, our cloning strategy targeted *PDR1*, a large protein of 1,068 amino acids, whose comprehensive mutagenesis would have been financially and technically challenging using conventional methods. To demonstrate the accuracy of our method, we focused on fragment 13 (F13; residues 301–325) of Pdr1, which combines both known and uncharacterized regions associated with drug resistance [27].

The *PDR1* F13 variant library was used to perform high-throughput functional screening of all possible amino acid substitutions, linking genotype to antifungal resistance phenotypes (Figure 2). The DMS experiment consisted of four main steps (Figure 2A): (i) generation of the *PDR1* variant library by transforming the plasmid library into a *S. cerevisiae* strain with doxycycline-repressible genomic *PDR1* expression (*ScPDR1-DOX*); (ii) competition assay with posaconazole; (iii) high-throughput sequencing; and (iv) fitness analysis of each variant.

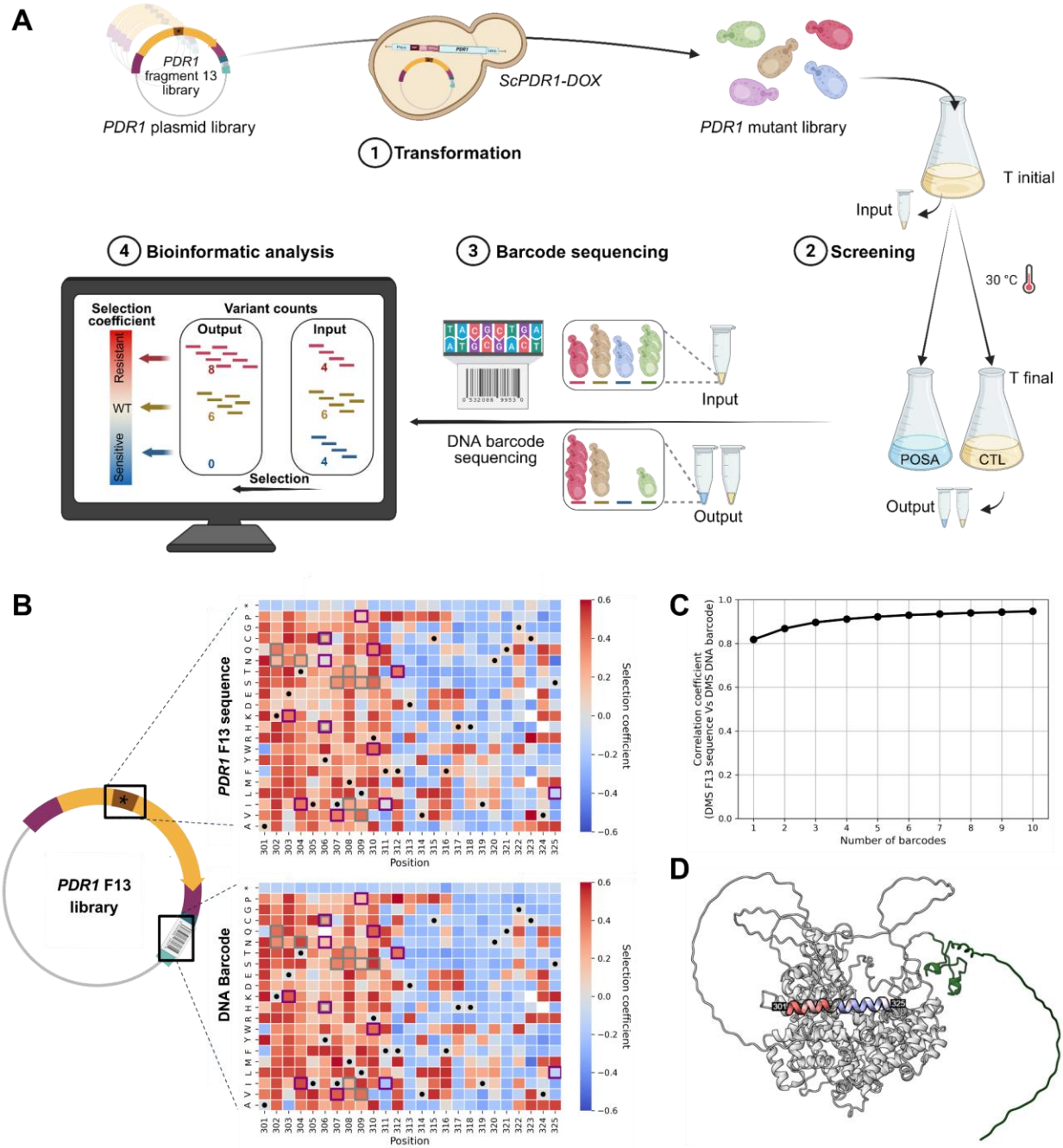

Figure 2 - Demonstration of the high-accuracy mutation profile obtained through barcode sequencing of a DMS plasmid library built from oPools.

A) Pooled competition workflow using our barcoded DMS plasmid library targeting a drug resistance hotspot t. 1. The *S. cerevisiae PDR1* variant library for F13 (residues 301-325) was transformed into a *S. cerevisiae* strain with a doxycycline-repressible endogenous *PDR1* expression (*ScPDR1-DOX*). **2.** Transformed strains expressing the variant library were grown in the presence of posaconazole (POSA, 0.40 µg/mL) or under drug-free control (CTL) conditions; **3.** High-throughput short-read sequencing of DNA barcodes. **4.** Selection coefficient analysis to identify resistant variants. **B) Azole resistance landscape of *PDR1* F13.** Heatmaps of selection coefficients for the 525 single amino acid variants screened, based on either direct sequencing of the mutated F13 region (top) or DNA-barcode inference (bottom). Squares in purple (*N. glabrata*)

and grey (*S. cerevisiae* or *S. paradoxus*) highlight azole resistance mutations previously reported [27]. Positive selection coefficients (>0, red) indicate increased fitness relative to the WT, while negative values (<0, blue) indicate reduced fitness. Black dots mark WT amino acids, and asterisks represent stop codons (as internal controls). Each value is the median of synonymous codons per amino acid. White cells indicate missing data. **C) Correlation between the selection coefficients measured with direct sequencing of the mutated F13 coding region and DNA-barcode inference**, as a function of the number of barcodes per variant considered. Means and confidence intervals were calculated from 100 random subsamplings per variant. **D) Pdr1 tertiary structure with DMS azole resistance landscape on F13 region.** Predicted tertiary structure of *S. cerevisiae* Pdr1 (AlphaFold 3 prediction, pTM = 0.72) shown in grey with its Zn_2Cys_6 DNA binding domain (residues 1-78) in green. The median selection coefficients from DMS are mapped onto the F13 (residues 301-325).

Although only short-read sequencing of DNA barcodes would normally be required, we performed full-length sequencing of the F13 sequence to compare the accuracy of the selection coefficients estimated from the barcode and the mutated fragment directly, as is routinely done for small genes [30–32] or through tile-seq for longer genes [13,33]. The estimates from the barcodes or from the F13 coding region were strongly correlated (r = 0.95, 10 barcodes). This high level of concordance was also observed with a much smaller number of barcodes (4 barcodes per mutation (r = 0.91)), confirming the robustness of our cloning and barcoding strategy (Figure 2C). By analysing selection coefficients across all amino acid substitutions, we identified two distinct regions within fragment F13 with different contributions to resistance (Figure 2B and D). Residues 301–312 showed frequent gain-of-resistance mutations and residues 313–324 appeared to play a limited role in resistance, with fewer substitutions conferring resistance.These results closely match resistance-conferring mutations reported in the literature for Pdr1 in both *S. cerevisiae* and the closely related species *N. glabratus* (Figure 2B; e.g., T304N, I307S, M308I, R310S, etc.) [27], supporting the power of our cloning strategy for mapping resistance landscapes for large proteins.

In summary, we developed an efficient, scalable, and cost-effective two-step cloning strategy for the construction of high-quality, barcoded DMS plasmid libraries for genes of any length. By combining affordable oPools, DNA barcodes, and optimized Gibson and Golden Gate assemblies, while using short-read sequencing to minimize financial costs, our method ensures high mutation coverage and barcode diversity that provide robust internal replicates, key parameters for accurate and reproducible mutational effects on fitness or resistance. This approach reduces both technical and financial barriers, facilitating its broader application across diverse gene sizes, biological systems, and experimental contexts. By supporting comprehensive genotype-phenotype analyses, this strategy strengthens functional genomics and mechanistic insights, and enhances the accessibility of these technologies across laboratories.

Methods

General information for plasmid and strain constructions and media

All cloning procedures were performed using *Escherichia coli* strain MC1061. *Saccharomyces cerevisiae* strain R1158, described in [34], served as the background for generating the doxycycline-repressible *S. cerevisiae PDR1* strain (*ScPDR1*-DOX, details below).

All antimicrobials were prepared as 1,000× stock solutions: ampicillin (AMP), doxycycline (DOX), geneticin (G418), and nourseothricin (NAT) were dissolved in sterile water, filtered, and stored at −20 °C; posaconazole (POSA) and itraconazole (ITR) were dissolved in dimethyl sulfoxide (DMSO) and also stored at −20 °C.

For bacterial liquid cultures, *E. coli* was grown in LB medium (0.5% yeast extract, 1% tryptone, 1% NaCl) at 37 °C with shaking at 250 rpm. For solid cultures, cells were grown on 2YT agar plates (1% yeast extract, 1.6% tryptone, 0.5% NaCl, 0.2% glucose, 2% agar) and incubated at 37 °C. When required, AMP was added at a final concentration of 100 µg/mL for plasmid selection. *S. cerevisiae* was cultured in YPD medium (1% yeast extract, 2% tryptone, 2% glucose) at 30 °C with shaking at 250 rpm. For solid cultures, 2% agar was added to YPD. Yeast transformants with pRS31N plasmids were selected on YPD plates supplemented with 100 µg/mL G418 and 100 µg/mL NAT.

All PCRs were performed using KAPA HiFi HotStart polymerase unless otherwise specified. Species, reagents, plasmids, computational tools and additional resources are listed in Supplementary Table B. Oligos are listed in Supplementary Table C, and PCR conditions, in Supplementary Table D.

The integrity of all assembled and mutagenized plasmids was verified either by Sanger sequencing (Plateforme de séquençage et de génotypage des génomes, Centre de recherche du centre hospitalier de Québec–Université Laval (CRCHUL), Canada) or by whole plasmid sequencing using Oxford Nanopore Technology with custom analysis and annotation (Plasmidsaurus, USA).

Plasmid library design

pRS31N-ScPDR1 WT

S. cerevisiae PDR1 (*PDR1*) was expressed from a yeast centromeric plasmid pRS31N-*ScPDR1* constructed as follows. First, a plasmid containing the *PDR1* sequence was created, including its promoter and terminator. The plasmid pRS31N containing AMP and NAT resistance markers was doubly digested with 20 U of both HindIII-HF and XbaI. The insert, a fragment containing *S. cerevisiae PDR1* native promoter (834 bp), coding sequence (3,207 bp) and terminator (345 bp), was amplified from the pMoBY-*ScPDR1* plasmid with primers adding homology to the pRS31N plasmid cloning site (PCR 1). The resulting PCR product corresponding to the insert was incubated for 1h30 at 37 °C with 10 U of DpnI enzyme to remove parental DNA. Subsequently,

the plasmid and insert were purified on magnetic beads and assembled by Gibson assembly to obtain pRS31N-*ScPDR1*.

As a BsaI restriction site is used in the construction of the *PDR1* deep mutational scanning (DMS) plasmid library, we had to remove three BsaI restriction sites in pRS31N--*ScPDR1*. The three sites were mutated by site-directed mutagenesis (site 1) or by homologous recombination with a short double-stranded DNA fragment (gBlock) corresponding to *PDR1* coding sequence between positions 2238 and 2720 without BsaI restriction sites (sites 2 and 3). The BsaI site 1 was removed by performing site-directed mutagenesis based on the QuickChange Site-Directed Mutagenesis System (Stratagene, La Jolla, CA). We amplified the pRS31N--*ScPDR1* plasmid using a pair of primers containing the desired mutation at the center (PCR 2). The PCR product was then incubated for 1h30 at 37 °C with 10 U of DpnI enzyme to remove parental DNA, and pRS31N--*ScPDR1* mutated plasmids (pRS31N--*ScPDR1* minus site 1) were retrieved directly by transformation in bacteria. For sites 2 and 3, the plasmid pRS31N-Sc*PDR1* minus site 1 was first PCR amplified (PCR 3). The resulting PCR product was incubated for 1h30 at 37 °C with 10 U of DpnI enzyme to remove parental DNA and then, purified on magnetic beads. Finally, the plasmid and gBlock insert were assembled by Gibson assembly to obtain pRS31N-*ScPDR1* WT. For clarity, throughout this study, pRS31N-*ScPDR1* WT refers to the plasmid after the BsaI site replacements, which served as the template for constructing the whole *PDR1* DMS plasmid library.

oPools

The DMS library was generated using only the *PDR1* coding sequence (CDS). Due to the limited length of synthetic DNA and to enable barcode-mutation association with short read sequencing, the 3,204 bp *PDR1* gene would be divided into 43 fragments of 75 bp each, except the last one which is of 54 bp. Fragment 1 goes from residue 1 to 25, fragment 2 goes from residue 26 to 50, and so on, up to the last fragment 43 (the smallest) going from residue 1050 to 1068. . We focused on fragments 13 as it is known to contain mutations causing drug resistance and also included fragment 43 to cover two sizes of inserts to be cloned between the mutated fragment and the barcode. For each fragment, a library was built using affordable pools of degenerate oligonucleotides (oPools). oPools are composed of three parts designed as follows (Figure 1A):

I. *PDR1* sequence of the fragment containing a single NNK codon (32 codons, including a stop codon);
II. BsaI module (two BsaI sites separated by CCGAAGCT to avoid self-dimerization); and
III. 30 bp DNA barcode with six random N and two fixed sequences (12 bp each) for each codon position. This design facilitates the identification of the mutated codon while allowing multiple distinct barcodes to represent the same mutation. As a result, each unique mutation is linked to several barcodes, providing internal replicates for downstream DMS analyses. oPools currently only allow for nine degenerate positions per DNA fragment. Three are used for the codon and six for the barcode.

We used a custom Python script to generate the oPool sequences. First, we ran generate_barcodes.py from the github.com/lzamparo/DNAbarcodes with the length option set at

12. This Python script generates all possible 12-nucleotide barcode sequences. We then randomized the barcode file, so sequences starting with the same nucleotides are not next to each other in the file. We used the Python script validate_barcodes.py (github.com/lzamparo/DNAbarcodes) on this randomized file to select 30,000 barcodes with a GC content between 40 and 60% and a hamming distance of 3 (validate_barcodes.py -input -output 30000 12 0.4 0.6 3). In a Jupyter notebook (barcode_identification_pdr1.ipynb), we removed barcodes in which BsaI was present to prevent any problem in the Golden Gate assembly step of our protocol. We also removed barcodes with two identical bases at the beginning or at the end to prevent stretches of the same bases. We split our filtered barcodes based on their GC content. We generated our 30 bp barcodes for the oPool by combining two 12 bp barcodes with six degenerate nucleotides, NN+barcode1+NN+barcode2+NN. We made sure the GC content of the sum of the two barcodes would be ~50%.

All oPool sequences were generated using a custom Jupyter notebook (opool_generator_20240212.ipynb). We cut the *PDR1* coding sequence into 75 bp fragments (25 codons per fragment) and we identified the 40-90 bp before and the 4 bp after each fragment. For each fragment, we generated 25 variant oligonucleotides in which a single codon was replaced by an NNK degenerate codon. Each oPool contains 25 different oligonucleotide sequences, each targeting one specific codon. The final sequences were generated by combining the 40-90 bp before the fragment, the NNK sequence, the 4 bp after the fragment, the BsaI module (GGAGACCgaagCTGGTCTCGACAG), one 30 bp barcode and the PBS_i7 (CTGTCTCTTATACACATCTCCGAGCCCACGAGAC).

All oPools are flanked by homology sequences at both the 5′ end (40 bp upstream of the target fragment within the *PDR1* sequence) and the 3′ end (PBS_i7 sequence, facilitating rapid sequencing library preparation), for a total of 186 to 258 bp per oPool. The complete list of oPool sequences used in this study is provided in Supplementary Table E.

Because cloning applications require double-stranded DNA inserts, oPools were amplified using two PCR reactions. The first PCR consisted of a single cycle using only the reverse primer (PCR 4). Since oPools are synthesized in the 5’ to 3’ direction, this initial step minimizes the incorporation of truncated oligos (linked to oPool incomplete synthesis) into the final product. The amplicons were purified using magnetic beads at a beads:DNA ratio of 1.8. Then, 2 µL of the purified product was used as template for a second PCR, involving both forward and reverse primers and limited to five cycles to reduce PCR-related errors (PCR 5). Each oPool amplification was performed in four replicates, which were pooled after the second PCR to maximize the diversity of variants carried into downstream cloning steps. This approach improved the overall quality of the oPools, ensuring sufficient insert quantity and diversity for subsequent steps of DMS library construction.

Plasmid library construction

Cloning strategy of the DMS plasmid library (Figure 1)

The cloning strategy was divided into two steps: Gibson assembly followed by Golden Gate assembly.

In the first step, the plasmid backbone was amplified from pRS31N-*ScPDR1* WT (PCR 6). The amplified region includes homology arms corresponding to the sequence upstream of the targeted fragment and extends to the plasmid region downstream of the terminator (i7 region). The resulting PCR product was incubated for 1h30 at 37 °C with 10 U of DpnI enzyme to remove parental plasmid DNA and then, purified using magnetic beads. The oPools are amplified as described in the "*oPools"* section. Backbone and insert fragments were assembled using Gibson assembly protocol [35]. To reach a target of ~25,000 transformants per fragment, necessary to ensure good barcode diversity and mutation coverage (Figure 1), multiple parallel Gibson reactions and transformations were performed for each fragment. Following transformations, 5 mL of 2YT medium was added directly onto each agar plate, and colonies were scraped using a sterile glass spreader. All transformants corresponding to a given fragment were pooled together. Aliquots were prepared, each corresponding to an optical density (OD_{600}) of 20 per fragment, and stored at -80 °C without (cell pellet) or with (glycerol stock) 15% glycerol. Plasmid libraries were extracted and purified from one cell pellet aliquot per fragment. These purified plasmids served as backbones for the subsequent cloning step.

In the second step, the *PDR1* missing 3′ end region, including the 3′ end coding sequence, terminator, and PBS_i5 (Figure 1A), was amplified (PCR 7). BsaI recognition sites were added to both ends of the amplicon to generate non-palindromic overhangs compatible with those in the Gibson-assembled plasmids. The resulting PCR product was incubated for 1h30 at 37 °C with 10 U of DpnI enzyme to remove parental DNA and then, purified on magnetic beads. The previously prepared plasmid libraries served as vectors, and the *PDR1* missing 3′ region acted as inserts for Golden Gate assembly, a one-pot cloning method alternating between BsaI digestion and ligation (PCR 8). To improve transformation efficiency, 5 µL of each Golden Gate reaction was transformed into NEB 5-alpha Competent *E. coli* cells following the manufacturer's instructions. Approximately 100,000 transformants per fragment were recovered, ensuring sufficient barcode diversity and adequate mutation coverage (Figure 1). To achieve this, multiple parallel Golden Gate reactions and transformations were performed for each fragment. Following transformation, 5 mL of 2YT medium was added directly to each agar plate, and colonies were scraped using a sterile glass spreader. All transformants corresponding to a given fragment were pooled together. Aliquots were prepared, each corresponding to an optical density (OD_{600}) of 80 per fragment, and stored at -80 °C without (cell pellet) or with (glycerol stock) 15% glycerol. Plasmid libraries were extracted and purified from one cell pellet aliquot per fragment. The resulting plasmid preparations corresponded to the final *PDR1* DMS plasmid libraries, with a distinct library for each *PDR1* fragment.

Plasmid library quality control by sequencing

At each cloning step, library quality was assessed by high-throughput sequencing, focusing on parameters such as mutation coverage and barcode diversity per mutation (Figure 1 - C and D).

First, low-quality reads were removed with *fastp* using default parameters -q 15 (the minimum phred score quality value that a base is qualified equal to 15) and -u 40 (40% of bases allowed to be unqualified). Reads were then merged with *bbmerge* from *bbmap*. All subsequent processing was done using custom Python scripts available at https://github.com/Landrylab/Jann_et_al_2025. To remove potential sequencing errors, the following reads were discarded: reads with incorrect length (reads including insertions or deletions), reads with more than one mutated codon within the *PDR1* coding region (75 bp), reads with unexpected mutations within barcode sequences, and reads with missing nucleotides within the *PDR1* or barcode sequence. After filtering, more than 60% and 80% of all reads were retained for F13 and F43, respectively.

Mutations with coverage of less than two reads were discarded. To measure the impact of combining results from multiple transformations (16 reactions, each with 5,000 (F13) or 7,500 (F43) transformants), we calculated the cumulative % of different metrics across all transformations sorted in a randomized manner. Means and confidence intervals were obtained for 100 random draws of transformation reactions. Metrics included: (i) informative barcodes; (ii) mutation coverage; barcode diversity for mutations represented by (iii) >4 barcodes and (iv) >9 barcodes. To standardize data, all metrics have been converted to the number of transformants/bp.

To perform sequencing-based quality control after Gibson assembly, we started with 20 ng of plasmid library obtained from bacteria minipreps. Sequencing libraries were prepared via three PCRs. The first two PCRs (PCR9 and PCR10) amplified the fragment of interest along with the downstream DNA barcode, while simultaneously adding the PBS_i5 adapter sequence at the 5′ end. The forward primer included the PBS_i5 and 20 bp upstream of the targeted region, while the reverse primer corresponds only to the PBS_i7. The amplicons were purified, diluted 1:1,000 and used as a template for a third PCR (PCR11), adding the appropriate Illumina i5 and i7 sample indexes for multiplexed sequencing. For each sample, the last PCR was performed in triplicate to maintain the diversity of the sequenced sample. All amplicons from the same sample were pooled and purified using magnetic beads. All samples were sent for high-throughput sequencing (Gibson sequencing sample descriptions are in Supplementary Table F).

Following Golden Gate assembly, only the DNA barcode region was sequenced, in order to verify that barcode diversity and mutation coverage were maintained. Because the PBS_i5 and PBS_i7 were already present on each side of the DNA barcode, sequencing libraries after Golden Gate assembly were generated in a single PCR (PCR12), which added the appropriate Illumina i5 and i7 sample indexes. Like after Gibson assembly, this PCR was also performed in triplicate per sample to prevent sampling bottlenecks. All replicate amplicons were pooled and purified on magnetic beads prior to sequencing. All samples were then sent for high-throughput sequencing (Golden Gate sequencing sample descriptions are in Supplementary Table G).

High-throughput sequencing was performed in paired-end 100 bp at the Centre de recherche du CHU de Québec – Université Laval sequencing platform (CHUL, Québec) using an Illumina NovaSeq 6000 S4 system. Libraries were sequenced at an average depth of ~250 reads per expected variant to assess barcode diversity and mutation coverage.

As done following the Gibson assembly, raw reads were filtered using *fastp* (default parameters), and overlapping paired-end reads were merged using *bbmerge.* Reads with incorrect length, unexpected barcode sequences, or missing nucleotides were removed, along with single-count reads. Barcode-mutation associations were performed by merging barcode reads from the Golden Gate assembly with the reference association generated after the Gibson assembly. To evaluate the library quality after the Golden Gate step, we re-calculated key metrics: informative barcodes, mutation coverage, and barcode diversity.

The presence of all expected mutations, with excellent DNA barcode diversity per mutation was confirmed in libraries F13 and F43 (after Gibson assembly : all mutations are covered by >4 barcodes and after Golden Gate assembly: ~93.6-100% of mutations are covered by >4 barcodes) (Figure 1C and D). A small number of mutations, specifically those at residues 322 to 324, were detected at lower read counts. Nevertheless, they still showed high mutation coverage (98.3%) and acceptable barcode diversity, with 71.7% of mutations with > 4 barcodes (Figure 1D), which is the threshold required for over 90% accuracy in selection coefficients (Figure 2C).

Variant library construction

Yeast strain construction (Supplementary Figure 2A)

The *ScPDR1*-DOX strain was generated based on the Yeast Tet-Promoters Hughes Collection (yTHC)[36]. The endogenous promoter of *PDR1* (spanning 50 bp upstream of the ATG codon; chrVIII:121683–121733) was replaced with a tetracycline-regulatable promoter. The KANMX-tetO7 cassette was amplified from plasmid pKB33 (PCR13) and introduced into competent *S. cerevisiae* R1158 cells using an adapted lithium acetate transformation protocol[37]. Transformants were selected on YPD medium containing 200 µg/mL G418.

Validation of genomic PDR1 expression control in ScPDR1-DOX (Supplementary Figure 2B)

To validate the control of genomic *PDR1* expression in the *ScPDR1*-DOX strain, *PDR1* expression levels were quantified in the presence and absence of doxycycline (DOX) in the culture medium. For this purpose, the gene coding for a monomeric enhanced Green Fluorescent Protein (*mEGFP*) was fused to the *PDR1* coding sequence in the genome of *ScPDR1*-DOX strain. The mEGFP sequence along with the hygromycin resistance module was amplified from plasmid pFA-*mEGFP-HPHNT1* (see construction below) using primers introducing homology arms targeting the 3′ end of the *PDR1* CDS and its terminator (PCR 14). Amplicons were treated with 20 U of DpnI for 1 h at 37 °C, purified using magnetic beads, and used to transform *ScPDR1*-DOX competent cells using the standard lithium acetate transformation protocol [37].

Yeast strains (*ScPDR1*-GFP-DOX and *ScPDR1*-DOX) were cultured overnight at 30 °C with shaking in synthetic complete (SC) medium in 24 deep-well plates. The SC medium contained 0.17% yeast nitrogen base without amino acids and ammonium sulfate, 0.1% monosodium glutamate, 2% glucose and amino acids drop-out without tryptophan. Saturated cultures were diluted to an OD_{600} of 0.15 in fresh medium with or without DOX (10 µg/mL), and grown again under agitation at 30 °C until reaching an OD_{600} of 0.5. Cells were then diluted to ~500 cells/µL in

0.2 µm filtered distilled water for flow cytometry analysis. GFP fluorescence was measured using a Guava easyCyte flow cytometer (MilliporeSigma) with excitation at 642 nm (GRN-B channel, 525/30 filter). A preliminary gating step (FSC-H (Forward Scatter Height) <15000 and FSC-A (Forward Scatter Area) <15000) was applied to select the main population of morphologically normal cells and to exclude non-representative events. A total of 5,000 events were recorded per replicate. Three independent biological replicates were analyzed per condition. Fluorescence signals were processed using a custom Python script and all the data (with control lacking GFP) are shown in Supplementary Figure 2B.

In order to generate *ScPDR1*-GFP-DOX yeast strain, we first had to construct pFA-*mEGFP-HPHNT1* plasmid. This was done by inserting *mEGFP* gene (insert 1) and *ENO1* terminator fragment (insert 2) into pFA-*hphNT1* (vector) using Gibson assembly. All three fragments were PCR amplified (PCR15, PCR16 and PCR17, respectively) and treated with 20 units of DpnI for 1 h at 37 °C before being purified on magnetic beads. Assembly was performed with the three fragments following a ratio of 1:5:5 (vector:insert 1: insert 2).

Yeast strain validation by complementation (Supplementary Figure 2C)

In order to validate whether *PDR1* expressed from the plasmid complements its genomic counterpart, we selected a condition where *PDR1* expression is beneficial (in presence of antifungal) and assessed the growth of *ScPDR1*-DOX strain transformed either with an empty plasmid or with one containing *PDR1* WT sequence. After adjusting cell density of precultures to an OD_{600} of 1, three serial 1/5 dilutions were prepared in 200 µL of water (i.e., 40 µL of cells in 160 µL of water). Then, 5 µL of each dilution were spotted on YPD + NAT agar plates supplemented with either 0.1% DMSO (control), 1 µg/mL ITR, 2 µg/mL ITR or 4 µg/mL ITR, in the presence or not of DOX (10 µg/mL). Plates were incubated at 30 °C for 48 h before imaging.

Library in yeast

The DMS plasmid library was introduced into *ScPDR1*-DOX yeast cells via lithium acetate transformation, performed fragment by fragment using a standard protocol [37]. For each fragment, approximately 100,000 colonies were recovered to ensure sufficient library coverage and barcode diversity. To collect transformants, 5 mL of YPD medium was added directly to each plate, and colonies were scraped using a sterile glass spreader. All transformants corresponding to a given fragment were pooled together. Aliquots were prepared, each corresponding to an optical density (OD_{600}) of 80 per fragment, and stored at −80 °C in 25% glycerol.

Pooled competition assay

A pooled competition assay was performed using the *PDR1* F13 variant library, in the presence or absence of an antifungal. All cultures were grown in YPD medium supplemented with NAT (100 µg/mL), to maintain plasmid selection, and DOX (10 µg/mL), to repress the endogenous *PDR1* promoter. As the used antifungal compound was dissolved in DMSO, the control condition also included 0.1% DMSO. Posaconazole (POSA) was used at a final concentration of

0.40 µg/mL, corresponding to the concentration that inhibits approximately 50% of wild-type growth, as previously reported [13].

The *PDR1* F13 variant library was first pre-cultured overnight in YPD + NAT, starting with an estimated inoculum of ~10,000 cells per variant (Time Point 0, TP0). Saturated cultures were diluted to an initial OD_{600} of 0.05 into fresh YPD + NAT + DOX + POSA, and grown until an OD_{600} of 0.80 was reached (TP1). A second dilution and growth cycle under the same conditions was performed (OD_{600} = 0.05 to 0.80), corresponding to a total of approximately eight mitotic generations (TP2). Identical conditions were used for the control (DMSO) condition.

At TP0, TP1 and TP2, cells were harvested by collecting 5 OD_{600} units per sample in 24 deep-well plate, followed by centrifugation at 916 × g for 5 min. Pellets were resuspended in 1 mL of YPD, transferred to 1.5 mL microcentrifuge tubes, and centrifuged again at 600 × g for 2 min. Supernatants were removed by aspiration, and resulting pellets were stored at −80 °C until plasmid extraction.

Plasmid recovery

Plasmid recovery from yeast was performed using the Zymoprep Yeast Plasmid Miniprep II kit, with the following modified protocol based on [13,19] to improve yield. Frozen cell pellets were resuspended in 200 µL of Solution 1, followed by the addition of 30 U of Zymolyase 20T. Cells were gently vortexed and incubated at 37 °C for 2 h. Following incubation, tubes were briefly vortexed and frozen at −80 °C for at least 20 min (up to overnight). After thawing at 37 °C for 3 min, 200 µL of Solution 2 was added and mixed, followed by the addition of 400 µL of Solution 3. Tubes were centrifuged at maximum speed for 3 min, and the supernatant (~800 µL) was transferred to a Zymo-Spin I column. Columns were washed with 550 µL of ethanol-containing wash buffer and centrifuged for 1.5 min at maximum speed. After removing the flow-through, columns were spun for an additional minute to dry. Plasmids were eluted by adding 10 µL of Tris buffer (10 mM, pH 8.0) and centrifuging for 1 min at maximum speed. Eluted DNA was stored at −20 °C until further processing.

High-throughput sequencing

Sequencing from yeast minipreps was performed using a protocol similar to that described in the *Plasmid library quality control by sequencing* section. Starting from 3 µL of yeast miniprep, an initial PCR was carried out to amplify only the *PDR1* from the plasmid using Phusion High-Fidelity DNA Polymerase and M13 primers flanking the *PDR1* insert on pRS31N (PCR18). This step avoids sequencing genomic *PDR1*.

From these PCR amplicons, two types of sequencing libraries were generated:

I. Direct sequencing of the F13 region of *PDR1*, and
II. Sequencing of DNA barcodes.

This dual approach allows us to validate whether barcode-predicted mutations corresponded accurately to the actual mutations present in the F13 sequence of *PDR1*.

For the F13 sequencing libraries, two rounds of PCR were performed. Starting with 2 µL of M13-purified amplicons, a first PCR made with Phusion High-Fidelity DNA Polymerase (PCR19) was used to amplify the F13 region while introducing PBS_i5 and PBS_i7 sequences at the 5′ and 3′ ends, respectively. In addition, a 0 to 3 nucleotides spacer (N) was added to the primers to increase sequencing diversity. A second PCR (PCR20) was then used to add the appropriate Illumina i5 and i7 sample indexes, as described in the *Plasmid library quality control by sequencing* section.

For the DNA barcode sequencing libraries, 2 µL of the M13-purified amplicons were used as a template for a single PCR reaction to add the appropriate Illumina i5 and i7 indexes (PCR21), as described in the *Plasmid library quality control by sequencing* section.

Both the F13 and DNA barcode sequencing libraries were sent for high-throughput sequencing in paired-end 150 bp at the Centre de recherche du CHU de Québec – Université Laval sequencing platform (CHUL, Québec) using an Illumina NovaSeq 6000 S4 system(DMS sequencing sample descriptions are in Supplementary Table H). All samples were sequenced to achieve a minimum of 500 reads per expected variant (i.e., ~0.4 million reads per sample for the F13 libraries and ~4 million reads per sample for the DNA barcode libraries). Only samples from timepoints TP0 and TP2 were sequenced. TP1 was excluded, as the limited frequency changes observed after just four generations hindered robust genotype-phenotype associations.

Data analysis

Selection coefficient and characterization of the variants

Selection coefficients were obtained with *gyōza*, a Snakemake-based workflow for the analysis of deep mutational scanning (DMS) data [38]. The pipeline includes adapter trimming with *Cutadapt*, read merging using *PANDAseq*, and clustering of identical reads via *VSEARCH*. Singleton reads (i.e., sequences observed only once) were excluded to reduce noise from sequencing errors. A custom script then aggregated read statistics across all processing steps.

The F13 samples were processed using the standard use of *gyōza*, with constant 20-bp sequences on either side of the mutated locus specified for trimming. For the barcoded library, specific steps of the workflow were run to obtain read counts for each barcode. The resulting table of read counts was merged to the table associating variants and barcodes (obtained in step 1). The modified table was input in the workflow to convert read counts into selection coefficients, keeping the barcode-level information. More specifically, the following steps were used to convert read counts into selection coefficients: (i) all read counts with depth >1, (ii) normalization by sample depth to obtain variant frequencies, (iii) calculation of $\log_2$ fold change between TP0 and TP2, (iv) normalization by the number of mitotic generations, and (v) subtraction of the median $\log_2$ fold-change of silent variants. To correct potential biases, normalization was performed using the median of variants encoding the wild-type amino acid sequence (excluding the wild-type nucleotide sequence).

Variants were assigned confidence scores based on their initial abundance at TP0 across replicates. A minimum threshold of five reads per mutation was used to define high-confidence variants, which were retained for downstream analysis. Selection coefficients were then aggregated by amino acid position, averaging across synonymous codons (Supplementary Tables I and J). The resulting tables were used to classify mutations from resistant to sensitive (0.6 to -0.6) based on their deviation from the WT. Finally, heatmaps were generated using the selection coefficient for each variant to enable clear visualization and comparison between F13 region and DNA barcode sequencing.

To assess the quality of the barcoded library, we compared the final selection coefficients per mutation obtained from sequencing of either mutated F13 region or DNA-barcode inference. To evaluate how barcode diversity influences the reliability of these coefficients, we progressively increased the number of barcodes required per mutation (from 1 to 10) and, at each level, performed 100 random samplings. For each sampling, we calculated the correlation between selection coefficients inferred from DNA barcodes and those obtained from the F13 region (Figure 2B).

Prediction and visualization of Pdr1 tertiary structure (Figure 2D)

As no experimentally determined structure was available for Pdr1 in the Protein Data Bank (PDB, RCSB), we used the AlphaFold 3 server [39] to predict its tertiary structure (pTM score = 0.72; seed = 264428788). The amino acid sequence of *S. cerevisiae* Pdr1 was obtained from UniProt (accession: P12383). Predicted structure was visualized using ChimeraX [40].

Data and materials availability

All data are available in the main text or the supplementary materials. Sequencing data are available in the NCBI Sequence Read Archive (SRA) under BioProject PRJNA1269095. All code and processed data to reproduce the analyses, results and figures are available at https://github.com/Landrylab/Jann_et_al_2025**.**

Acknowledgements
We thank Dan Evans-Yamamoto, Philippe Després and other Landrylab members for discussions and feedback on the design of the cloning strategy.

Funding
This work was supported by a Genome Québec and Genome Canada grant (6569), a Canadian Institutes of Health Research (CIHR) Foundation grant (387697), a CIHR project grant (202409PJT), and a Natural Sciences and Engineering Research Council of Canada (NSERC) CREATE grant (EvoFunPath) to CRL. JJ and RD are supported by postdoctoral fellowships from NSERC. JJ benefits also from FRQS postdoctoral fellowship (343898). CRL holds the Canada Research Chair in Cellular Systems and Synthetic Biology.

Authors' contributions

AKD, JJ, IGA, CRL designed the experimental strategy; JJ & IGA performed experiments; JJ, IGA, AP, AF and RD performed the data analysis; JJ wrote the manuscript with input from IGA and CRL; All authors read and commented on the manuscript; CRL and IGA supervised and administered the project; CRL obtained funding.

Supplementary Figures:

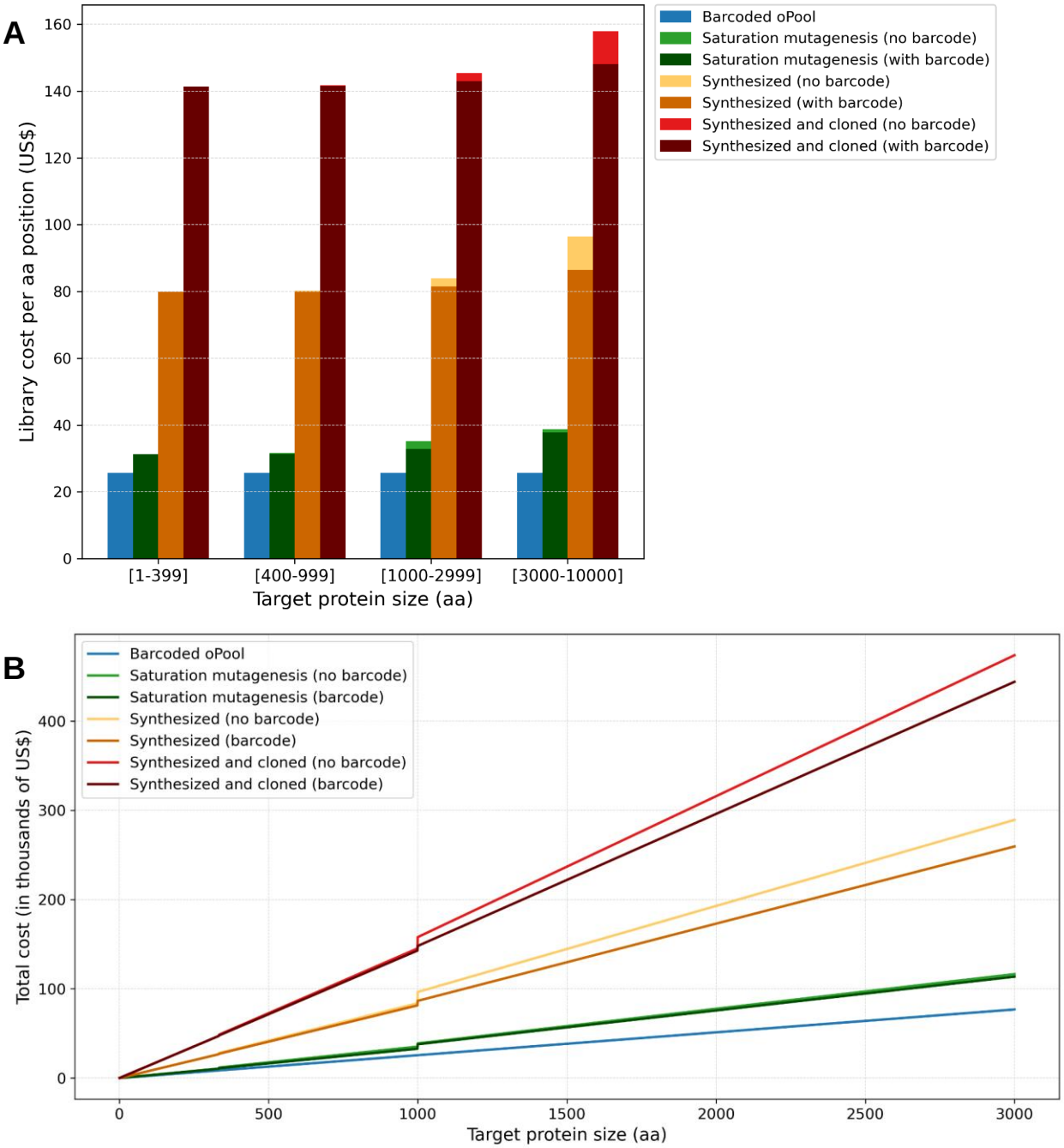

Supplementary Figure 1: Cost comparison of different strategies for constructing NNK-based DMS plasmid libraries. Approaches include saturation mutagenesis, commercial gene synthesis, and the barcoded oPool cloning strategy developed in this study, each evaluated with and without barcodes. **A)** Library cost per amino acid position across DMS library strategies and target protein sizes. **B)** Total projected cost of DMS libraries as a function of target protein size. All costs include nucleotide synthesis (e.g., primers, oPools, or complete library), cloning steps, and sequencing for both library validation and a typical one-condition functional assay experiment (Supplementary Table A). Barcoded library costs are based on having four barcodes per mutation, corresponding to the 90% accuracy threshold described in this study (Figure 2C).

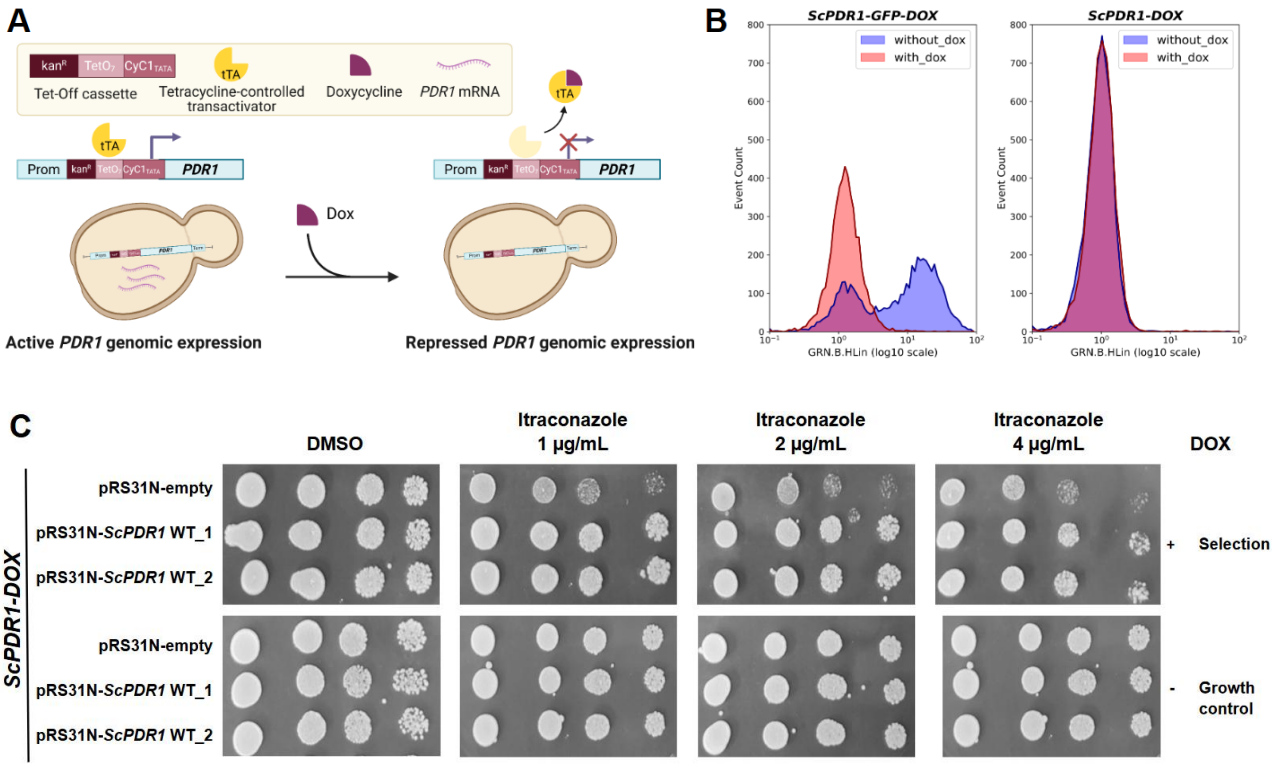

Supplementary Figure 2: Construction and validation of a *S. cerevisiae* strain to measure the impact of *PDR1* mutations on drug resistance. A) Inducible control of genomic *PDR1* expression in *S. cerevisiae* using a doxycycline-repressible Tet-Off promoter in the ScPDR1-DOX background. **B)** Validation of genomic *PDR1* repression in the *ScPDR1*-DOX strain. *PDR1* expression level was assessed by flow cytometry using a GFP fusion as a reporter. Fluorescence intensity is shown for the strain expressing GFP (left panel: *ScPDR1-GFP-DOX*) and the negative control strain without GFP (right panel: *ScPDR1-DOX*) in media with (red) or without (blue) DOX. GFP intensity was analyzed on the main population of morphologically normal cells (FSC-H<15000 and FSC-A<15000). 5,000 events were recorded per replicate. Three independent biological replicates were analyzed per condition. **C)** Spot dilution complementation assay of genomic *PDR1* expression in *ScPDR1-DOX* by plasmid-expression of *ScPDR1* (pRS31N-*ScPDR1* WT) or not (pRS31N-empty (control)). Growth conditions : DMSO (control) or Itraconazole (antifungal).

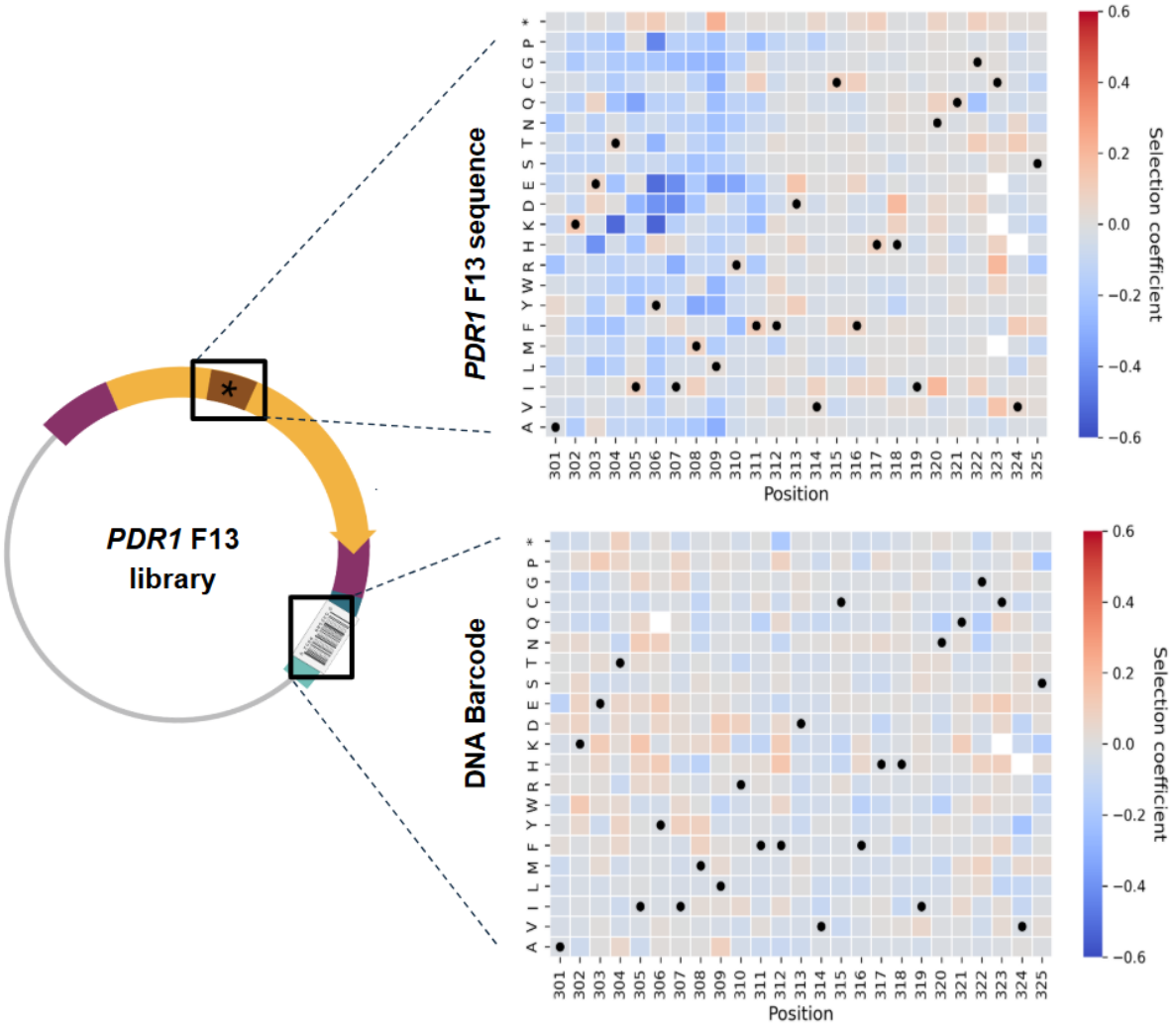

Supplementary Figure 3 : Fitness landscape of *PDR1* F13 in control condition (DMSO). Heatmaps of selection coefficients for the 525 single amino acid variants screened, based on either direct sequencing of the mutated F13 region (top) or DNA-barcode inference (bottom). Positive selection coefficients (>0, red) indicate increased fitness relative to the WT, while negative values (<0, blue) indicate reduced fitness. All selection coefficients for each amino acid position are provided in Supplementary Tables I and J. Black dots mark WT amino acids, and asterisks represent stop codons (as internal controls). Each value is the median of synonymous codons per amino acid. White cells indicate missing data.

References

1. Fowler, D. M. & Fields, S. Deep mutational scanning: a new style of protein science. *Nat. Methods* **11**, 801–807 (2014).
2. Wei, H. & Li, X. Deep mutational scanning: A versatile tool in systematically mapping genotypes to phenotypes. *Front. Genet.* **14**, 1087267 (2023).
3. Kitzman, J. O., Starita, L. M., Lo, R. S., Fields, S. & Shendure, J. Massively parallel single-amino-acid mutagenesis. *Nat. Methods* **12**, 203–6, 4 p following 206 (2015).
4. Wrenbeck, E. E. *et al.* Plasmid-based one-pot saturation mutagenesis. *Nat. Methods* **13**, 928–930 (2016).
5. Stiffler, M. A., Hekstra, D. R. & Ranganathan, R. Evolvability as a function of purifying selection in TEM-1 β-lactamase. *Cell* **160**, 882–892 (2015).
6. Fowler, D. M. *et al.* High-resolution mapping of protein sequence-function relationships. *Nat. Methods* **7**, 741–746 (2010).
7. Matreyek, K. A. *et al.* Multiplex assessment of protein variant abundance by massively parallel sequencing. *Nat. Genet.* **50**, 874–882 (2018).
8. Findlay, G. M. *et al.* Accurate classification of BRCA1 variants with saturation genome editing. *Nature* **562**, 217–222 (2018).
9. Sadhu, M. J. *et al.* Highly parallel genome variant engineering with CRISPR-Cas9. *Nat. Genet.* **50**, 510–514 (2018).
10. Howard, C. J. *et al.* High resolution deep mutational scanning of the melanocortin-4 receptor enables target characterization for drug discovery. (2025) doi:10.7554/elife.104725.2.
11. Dadonaite, B. *et al.* Spike deep mutational scanning helps predict success of SARS-CoV-2 clades. *Nature* **631**, 617–626 (2024).

12. Shepherdson, J. L. *et al.* Mutational scanning of CRX classifies clinical variants and reveals biochemical properties of the transcriptional effector domain. *Genome Res.* **34**, 1540–1552 (2024).
13. Bédard, C. *et al.* Most azole resistance mutations in the Candida albicans drug target confer cross-resistance without intrinsic fitness cost. *Nat. Microbiol.* **9**, 3025–3040 (2024).
14. Kinsler, G. *et al.* Extreme sensitivity of fitness to environmental conditions: Lessons from #1BigBatch. *J. Mol. Evol.* **91**, 293–310 (2023).
15. Maes, S., Deploey, N., Peelman, F. & Eyckerman, S. Deep mutational scanning of proteins in mammalian cells. *Cell Rep. Methods* **3**, 100641 (2023).
16. Fowler, D. M. *et al.* An Atlas of Variant Effects to understand the genome at nucleotide resolution. *Genome Biol.* **24**, 147 (2023).
17. Maciá Valero, A., Prins, R. C., de Vroet, T. & Billerbeck, S. Combining oligo pools and Golden Gate cloning to create protein variant libraries or guide RNA libraries for CRISPR applications. *Methods Mol. Biol.* **2850**, 265–295 (2025).
18. Kuiper, B. P., Prins, R. C. & Billerbeck, S. Oligo pools as an affordable source of synthetic DNA for cost-effective library construction in protein- and metabolic pathway engineering. *Chembiochem* **23**, e202100507 (2022).
19. Starr, T. N. *et al.* Deep mutational scanning of SARS-CoV-2 receptor binding domain reveals constraints on folding and ACE2 binding. *Cell* **182**, 1295–1310.e20 (2020).
20. Weile, J. *et al.* Pacybara: accurate long-read sequencing for barcoded mutagenized allelic libraries. *Bioinformatics* **40**, (2024).
21. Fisher, M. C. *et al.* Tackling the emerging threat of antifungal resistance to human health. *Nat. Rev. Microbiol.* **20**, 557–571 (2022).
22. Berman, J. & Krysan, D. J. Drug resistance and tolerance in fungi. *Nat. Rev. Microbiol.* **18**, 319–331 (2020).
23. Langner, S., Staber, P. B. & Neumeister, P. Posaconazole in the management of refractory

invasive fungal infections. *Ther. Clin. Risk Manag.* **4**, 747–758 (2008).

24. Boutin, C.-A. & Luong, M.-L. Update on therapeutic approaches for invasive fungal infections in adults. *Ther. Adv. Infect. Dis.* **11**, 20499361231224980 (2024).
25. Maquera-Afaray, J. *et al.* Antifungal prophylaxis with posaconazole in immunocompromised children younger than 13 years. *J. Pediatr. Pharmacol. Ther.* **27**, 57–62 (2022).
26. Pardiwala, A., Datarkar, A. N., Manekar, V. & Daware, S. Posaconazole as single or adjunctive antifungal in mucormycosis of the maxilla: systematic review and meta-analysis. *J. Oral Med. Oral Surg.* **29**, 41 (2023).
27. Bédard, C. *et al.* FungAMR: A comprehensive portrait of antimicrobial resistance mutations in fungi. *bioRxiv* (2024) doi:10.1101/2024.10.07.617009.
28. Gale, A. N. *et al.* Redefining pleiotropic drug resistance in a pathogenic yeast: Pdr1 functions as a sensor of cellular stresses in Candida glabrata. *mSphere* **8**, (2023).
29. Ferrari, S. *et al.* Gain of function mutations in CgPDR1 of Candida glabrata not only mediate antifungal resistance but also enhance virulence. *PLoS Pathog.* **5**, e1000268 (2009).
30. Cisneros, A. F. *et al.* Epistasis between promoter activity and coding mutations shapes gene evolvability. *Sci Adv* **9**, eadd9109 (2023).
31. Dibyachintan, S. *et al.* Cryptic genetic variation shapes the fate of gene duplicates in a protein interaction network. *Nat. Commun.* **16**, 1530 (2025).
32. Domingo, J., Diss, G. & Lehner, B. Pairwise and higher-order genetic interactions during the evolution of a tRNA. *Nature* **558**, 117–121 (2018).
33. Weile, J. *et al.* A framework for exhaustively mapping functional missense variants. *Mol. Syst. Biol.* **13**, 957 (2017).
34. Hughes, T. R. *et al.* Functional discovery via a compendium of expression profiles. *Cell* **102**, 109–126 (2000).
35. Gibson, D. G. *et al.* Enzymatic assembly of DNA molecules up to several hundred

kilobases. *Nat. Methods* **6**, 343–345 (2009).

36. Mnaimneh, S. *et al.* Exploration of essential gene functions via titratable promoter alleles. *Cell* **118**, 31–44 (2004).
37. Gietz, R. D. & Schiestl, R. H. High-efficiency yeast transformation using the LiAc/SS carrier DNA/PEG method. *Nat. Protoc.* **2**, 31–34 (2007).
38. Durand, R., Pageau, A. & Landry, C. R. gyōza: a Snakemake workflow for modular analysis of deep-mutational scanning data. *bioRxiv* (2025) doi:10.1101/2025.02.19.639168.
39. Abramson, J. *et al.* Accurate structure prediction of biomolecular interactions with AlphaFold 3. *Nature* **630**, 493–500 (2024).
40. Meng, E. C. *et al.* UCSF ChimeraX: Tools for structure building and analysis. *Protein Sci.* **32**, e4792 (2023).